Mg-Rich Authigenic Carbonates in Coastal Facies of the Vtoroe Zasechnoe Lake (Southwest Siberia): First Assessment and Possible Mechanisms of Formation

Andrey A. Novoselov [1], Alexandr O. Konstantinov [2,*], Artem G. Lim [3], Katja E. Goetschl [4], Sergey V. Loiko [3,5], Vasileios Mavromatis [4,6] and Oleg S. Pokrovsky [6,7]

[1] Institute of Earth Sciences, University of Tyumen, Tyumen 625002, Russia; mr.andreygeo@mail.ru
[2] Center of Advanced Research and Innovation, Tyumen Industrial University, Tyumen 625000, Russia
[3] BIO-GEO-CLIM Laboratory, National Research Tomsk State University, Tomsk 634050, Russia; lim_artyom@mail.ru (A.G.L.); s.loyko@yandex.ru (S.V.L.)
[4] Institute of Applied Geosciences, Graz University of Technology, Graz 8010, Austria; katja.goetschl@tugraz.at (K.E.G.); vasileios.mavromatis@get.omp.eu (V.M.)
[5] Tomsk Oil and Gas Research and Design Institute (TomskNIPIneft), Tomsk 634027, Russia
[6] Géosciences Environnement Toulouse (GET), CNRS, UMR 5563, 31400 Toulouse, France; oleg.pokrovsky@get.omp.eu
[7] N.P. Laverov Federal Center for Integrated Arctic Research (FCIArctic), Russian Academy of Sciences, Arkhangelsk 163000, Russia
* Correspondence: konstantinov.alexandr72@gmail.com; Tel.: +7-982-782-3753

Abstract: The formation of Mg-rich carbonates in continental lakes throughout the world is highly relevant to irreversible CO_2 sequestration and the reconstruction of paleo-sedimentary environments. Here, preliminary results on Mg-rich carbonate formation at the coastal zone of Lake Vtoroe Zasechnoe, representing the Setovskiye group of water bodies located in the forest-steppe zone of Southwest Western Siberia, are reported. The Setovskiye lakes are Cl^-–Na^+–(SO_4^{2-}) type, alkaline, and medium or highly saline. The results of microscopic and mineralogical studies of microbialites from shallow coastal waters of Lake Vtoroe Zasechnoe demonstrated that Mg in the studied lake was precipitated in the form of hydrous Mg carbonates, which occur as radially divergent crystals that form clusters in a dumbbell or star shape. It is possible that hydrous Mg carbonate forms due to the mineralization of exopolymeric substances (EPS) around bacterial cells within the algal mats. Therefore, the Vtoroe Zasechnoe Lake represents a rare case of Mg-carbonates formation under contemporary lacustrine conditions. Further research on this, as well as other lakes of Setovskiye group, is needed for a better understanding of the possible role of biomineralization and abiotic mechanisms, such as winter freezing and solute concentration, in the formation of authigenic Mg carbonate in modern aquatic environments.

Keywords: Western Siberia; Mg carbonates; Mg-Ca carbonates; hydromagnesite; lakes; biomineralization

1. Introduction

The physicochemical parameters controlling the formation of Mg-carbonates, and especially, magnesite ($MgCO_3$), make up one of the most controversial scientific topics in biogeochemistry, mineralogy, and the geology of sedimentary rocks [1]. Similar to the formation of dolomite ($CaMg(CO_3)_2$) [2–6], the abiotic precipitation of magnesite at the Earth-surface pressures, as well as the temperatures, is kinetically limited due to the strongly pronounced hydrophilic properties of the Mg^{2+} ion [7–9]. Instead, hydrated metastable phases, such as nesquehonite ($MgCO_3 \cdot 3H_2O$), dypingite

($Mg_5(CO_3)_4(OH)_2 \cdot 5H_2O$), and hydromagnesite ($Mg_5(CO_3)_4(OH)_2 \cdot 4H_2O$) are formed under conditions of modern playas and continental water bodies [10]. At the same time, the ancient sedimentary strata are composed of magnesite, which is the most stable Mg-carbonate mineral phase [11,12]. Therefore, the question about the possible mechanism of magnesite formation is still debatable: Is it formed by the decomposition/aging of the hydrated phase of metastable compounds such as hydromagnesite [13], or is it the primary precipitation product [14]?

Another interesting aspect of this problem is related to the fact that most of the examples of Mg-carbonate formation under modern conditions are associated with algal mats [12,15,16], which in turn suggests that biomineralization is the main factor in their formation. The results of field studies and laboratory experiments demonstrated that the metabolic activity of microorganisms plays a crucial role in the precipitation of hydrous Mg-carbonates in modern aquatic environments [16–18].

In contrast to the vast literature related to the precipitation of Ca-carbonates and Ca–Mg-carbonates by living organisms [4,19–27], the biomineralization of Mg-carbonates has been studied to a far lesser extent [12]. However, this process can provide important insights into dolomite formation and can be key to understanding the fundamental mechanisms of the evolution of the biosphere in the early stages of its development [1]. Another practical aspect related to the problem of Mg-carbonate precipitation is the possibility of using the data obtained during field observations and laboratory experiments to develop efficient carbon sequestration (mineralization) technologies [28–30].

Numerous examples of modern Mg-carbonate formation under conditions of playas and saline continental lakes were reported for various arid and semi-arid regions of the world [12,14,15,31–45]. The majority of such environments are evaporitic and/or alkaline [12], which is most often related to specific climatic conditions and the specific geology of territories where such phenomenon appear. For example, in the case of hydromagnesite playas of British Columbia in Canada and saline Lake Salda in Turkey, the source of Mg is related to the weathering of ultrabasic rocks [16,46,47]. In general, however, the formation of Mg-carbonates rarely prevails over the formation of Ca and Ca–Mg-carbonates and such environments can be considered as unique natural objects.

The territory of the South of Western Siberia and Northern Kazakhstan is one of the largest drainless basins (having no connection to the sea) in the world. The territory of Southwestern Siberia belongs to the Northern part of the Central Asian endorheic basin, which occupies the territory of 2.4 million km^2 (146 thousands km^2 within the territory of Russia) [48]. Lakes are highly abundant in the landscapes of this region and the processes of modern carbonate formation is an important component in their functioning as biogeochemical systems. Most studies devoted to mineral formation in continental water bodies of Western Siberia indicate that calcite, aragonite, Mg-calcite, and Ca-dolomite are the most common authigenic carbonates in such environments [49–53], while Mg-carbonates are quite rare and appear in small quantities [54]. In contrast, the lakes in the forest-steppe of the Trans-Ural region located in the Southwestern part of Western Siberia are reported to precipitate Mg-carbonates, which predominate over Ca- and Ca–Mg-carbonates [33]. These water bodies belong to the areas covered with Neogene and Quaternary continental deposits, but large masses of ultrabasic rocks of the Urals are located at a considerable distance from this area and accordingly, the source of high Mg contents in the water of some Trans-Ural lakes remains unclear. Overall, the carbonate formation in forest-steppe lakes in the Southwestern part of Western Siberia are practically not studied, with the exception of one work [33], which contains a brief report on the occurrence of Mg-rich carbonates in the upper layer of the bottom sediments of some Setovskiye group lakes.

The two main objectives of this study are: (1) The microscopic and mineralogical characterization of Mg-rich carbonates found in the coastal areas of one of the lakes from the Setovskiye group (forest-steppe zone of the Southwest of Western Siberia); (2) the identification of chemical and morphological features related to biogenic precipitation of Mg-carbonates, as well as the explanation of possible mechanisms of this process.

2. Materials and Methods

2.1. Geographical and Geological Settings

The Setovskiye lakes include eight drainless (no outlet) water bodies, the largest of which are Krugloe, Dolgoe, Pervoe Zasechnoye, Vtoroe Zasechnoye, and Solenoe. The typical depth of the lakes is between 1 and 3 m. The studied water bodies are located 40 km Southwest of the Kurtamysh town (Kurgan Region, Russia; Figure 1). The lakes are located within the Southwestern peripheral part of the West Siberian Plain and belong to the Northern forest-steppe zone of the Trans-Ural Region [55]. Quaternary deposits within the study area are limnic and limno-alluvial sediments of the Uysko-Uboganskaya formation (LIIuu, up to 15 m) and carbonate loess deposits of the Zyryansky horizon (LIIIzr). Quartz Neogene sands of the Naurzumskaya formation underlie quaternary sediments [56]. The Tobol River and its tributaries divide the territory of the forest steppe Trans-Urals into several weakly drained interfluves, whose watersheds contain numerous lakes.
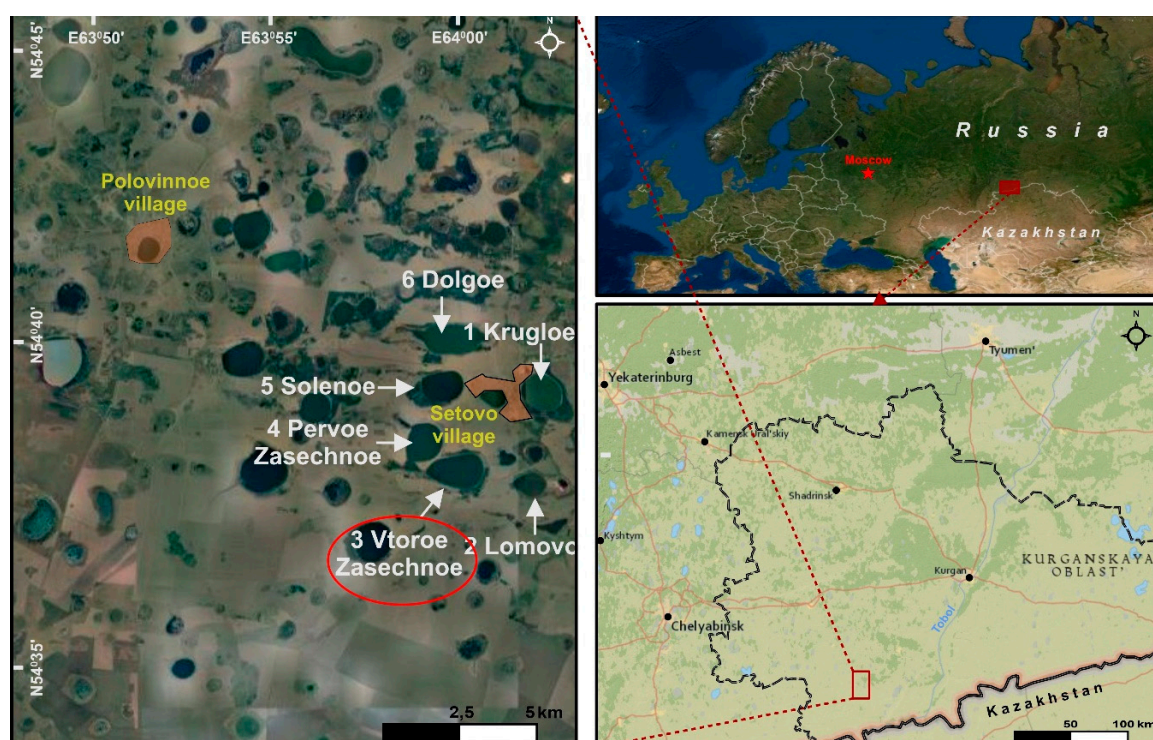
Figure 1. Location of the Setovskiye Lakes within the territory of Northern Eurasia and Trans-Urals; the numeration of lakes is given, as in Table 1.

The climate of the territory is moderately continental. The average annual temperature is 1.9 °C and the average annual precipitation is 381 mm [57]. The rainfall mainly feeds the water bodies in warm seasons and the snowmelt provides water in spring; however, the ground waters input may also contribute to the water balance in some cases. The landscapes of the territory surrounding the Setovskiye lakes are represented by the alternation of plowed fields and birch groves, with a predominance of Chernozems on watersheds and Planosols in depressions, which is typical for the Northern forest-steppe ecotone [58]. The agriculture represents the main source of anthropogenic impact on the environment within the area.

2.2. Field Study and Sampling

Water samplings of six lakes from Setovskiye group were carried out from 28 to 30 September 2018 (Figure 1). This sampling period corresponds to a summer baseflow of the region, which is

representative of the major period of authigenic carbonate mineral formation. Based on the results of preliminary observations, the coastal facies of the Lake Vtoroe Zasechnoye, where algae mats and microbialites were found during field studies, were selected for detailed sampling and analyses. The algal mats appeared as dense layers of dried cemented and partly mineralized algae formed in the shoreline, while small greenish and creamy decaying microbialites cemented by carbonate material appeared within the shallow water (Figure 2). The dried samples were used for mineralogical studies via scanning electron microscopy (SEM) and for the preparation of transparent thin sections for optical microscopic observations.
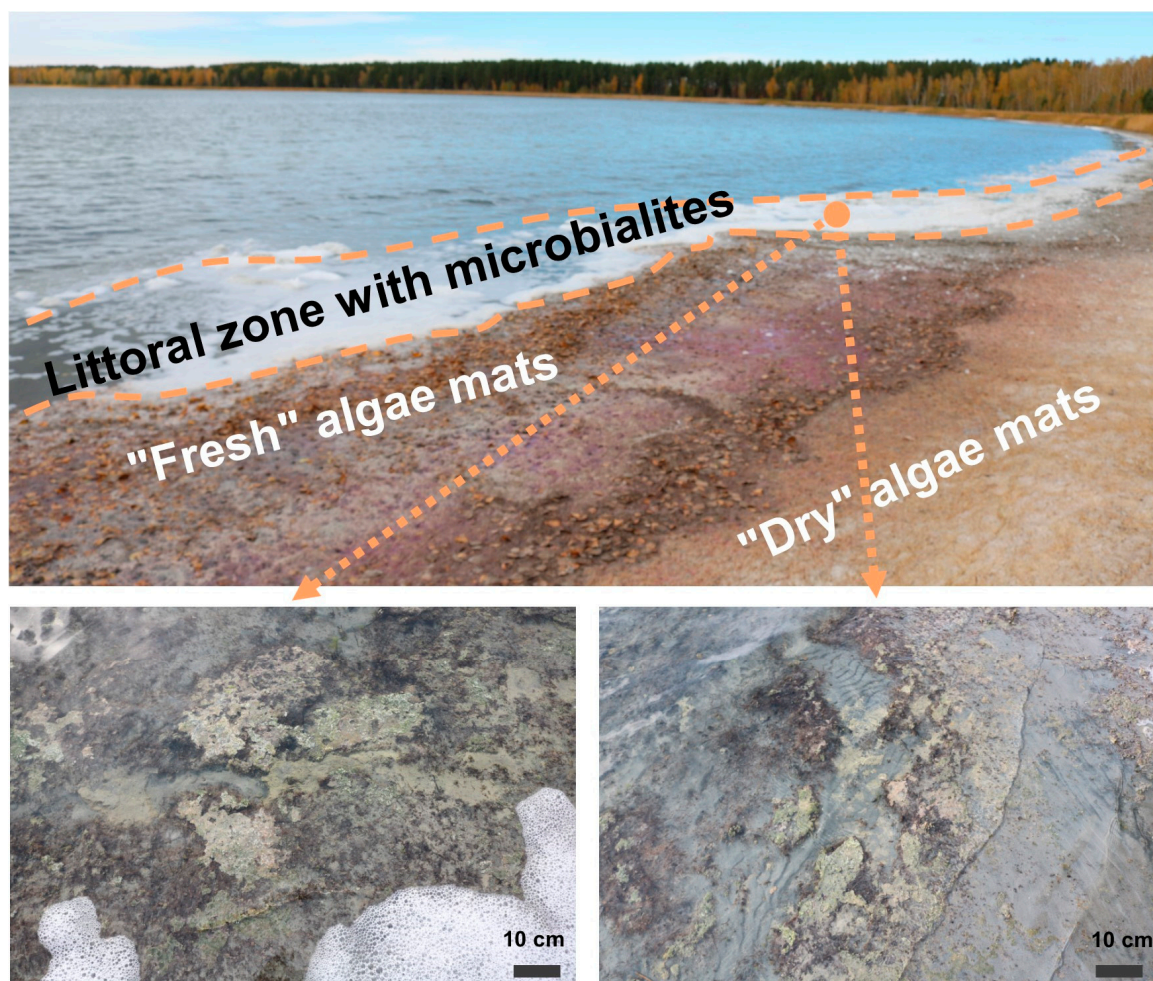
Figure 2. Scheme illustrating the near-shore facies of Vtoroe Zasechnoe Lake from the Setovskiye group of water bodies.

Water samples were taken from six main lakes representing the Setovskiye group. The pH, specific electric conductivity, and temperature were measured in the field using a Multi 3420 portable multiparameter meter (WTW, Xylem Analytics, Germany). Samples of lake waters were filtered on-site through disposable MILLEX Filter units (0.45 µm pore size, 33 mm in diameter) using a sterile plastic syringe and vinyl gloves. The first 20–50 mL of filtrate was discarded and the subsequent filtrate was collected into pre-washed 250 mL polypropylene bottles. Filtered samples of lake waters were taken in two bottles, one was acidified with bidistilled nitric acid to a concentration of 2% for the analysis of cations and trace elements, and the second was not acidified and used for analyses of dissolved organic (DOC) and inorganic (DIC) carbon and anions following standard techniques used in the Géosciences Environment Toulouse Laboratory [59]. Before analyses, filtered samples were stored in a refrigerator at 4–6 °C.

2.3. Analytical Methods

Hydrochemical studies of water samples from six lakes representing the Setovskiye group included measurements of DOC, DIC, cations, Cl^-, and SO_4^{2-}. The major anion concentrations (Cl^- and SO_4^{2-}) were analyzed by ion chromatography (Dionex 2000i, Thermo Fisher Scientific, Waltham, MA, USA) with an uncertainty of 2%. The dissolved organic carbon (DOC) and dissolved inorganic carbon (DIC) were determined using a TOC-Vscn analyzer (Shimadzu, Kyoto, Japan) with an uncertainty of 3% and a detection limit of 0.1 mg/L. The major elements were measured by quadrupole Agilent 7500ce ICP-MS system (Agilent Technologies, Santa Clara, CA, USA) with an uncertainty of ±5%. Indium and rhenium were used as internal standards. The international geostandard SLRS-5 (Riverine Water Reference Material for Trace Metals, certified by the National Research Council of Canada) was used to check the validity and reproducibility of each analysis.

The primary diagnostics of collected samples was carried out using a Leica EZ4 D stereomicroscope (Leica Microsystems, Wetzlar, Germany) with an integrated digital camera. The studies of 10 representative samples were performed in thin sections of dried microbialites and algae mats using an Eclipse LV100POL polarization microscope (Nikon, Tokyo, Japan) and an Axio Vert reflected light microscope (Carl Zeiss, Oberkochen, Germany). The SEM-EDS analysis was performed using a TM3000 scanning electron microscope (Hitachi, Tokyo, Japan) with a Quantax 70 EDS attachment (Bruker, Billerica, MA, USA) at X100–5000 magnification and a JSM-6390LV scanning electron microscope (Jeol, Tokyo, Japan) with an INCA Energy 450 X-Max80 EDS attachment (Oxford Instruments, Abingdon, UK). The SEM observation were made under high vacuum (HV-mode), mainly in the elemental composition mode (BSE, registration of back scattered electrons). While performing the EDS analysis, the voltage was 15 and 20 kV for the first and second devices, respectively.

Confocal laser-scanning microscopy (CLSM) is often used to identify signs related to the activity of living organisms within stromatolites and microbialites [25,60,61]. Selected thin sections of algae mats and microbialites were examined using a Zeiss LSM 780 NLO confocal laser-scanning microscope (Carl Zeiss, Oberkochen, Germany). Lasers with wavelengths of 405, 488, and 561 nm were used as a source of fluorescence excitation in a microscope. Images illustrating the fluorescence of the studied samples were collected using an emission filter that transmits light with a wavelength between 505 and 539 nm (visible, green).

The mineralogical composition of the collected solid samples (two for microbialites and two for algal mats) was examined by a powder X-ray diffraction (XRD) technique. Diffractograms were recorded by a PANalytical X'Pert PRO diffractometer (Malvern Panalytical, Malvern, UK) using Co-Kα-radiation (40 mA, 40 kV) at a 2θ range from 5° to 85° and a scan speed of 0.03 °s^{-1}. Malvern Panalytical's HighScore Plus software with the ICSD database was used for the qualitative characterization of the crystalline products, and the mineral phases were quantified by Rietveld refinement. Corundum standards were always used to constrain the calibration. Analytical uncertainty of the quantification was within 1 wt.%.

Thermodynamic modeling included the calculation of saturation indices of aqueous solution with respect to various carbonates using the Visual MINTEQ ver. 3.1 software package [62]. The parameters including pH, temperature, and the concentrations of individual ions obtained from the measurements of these values in field and laboratory conditions were used as input parameters.

3. Results

3.1. Water Chemistry of Setovskiye Lakes

The physical and chemical parameters of the studied lakes (Table 1) indicate that all lakes belong to the group of small, closed-water reservoirs with depths varying from 1.1 to 2.3 m. The lake waters are alkaline (pH values from 9.0 to 9.7); moderately or strongly saline (TDS values varied from 28 to 84 g/L) and belong to the Cl^-–Na^+–(SO_4^{2-}) type. The Mg/Ca molar ratio in studied lakes varied from 38 to 66, except for Lakes Krugloe (9.3) and Vtoroe Zasechnoe (100), where these values were

significantly lower and higher, respectively, than most of the Setovskiye Lakes. The microbialites were found only in the coastal zone of the Vtoroe Zasechnoe Lake, exhibiting the highest Mg/Ca ratio. The DOC and DIC concentrations varied from 69 to 112 and 240 to 365 mg/L, respectively. These results demonstrated significant spatial variability in hydrochemical parameters (notably salinity and Mg/Ca molar ratio) within the same group of closely located lakes. Note that the reasons of very high Mg/Ca ratios in some water bodies, as well as the variability of this parameter for the whole group cannot be explained based on the results of preliminary studies.

Table 1. Physical and chemical parameters of studied lakes of the Setovskiye group.

No.	Lake	Coordinates		Surface Area (km^2)	Watershed Surface (km^2)	Mean Depth (m)	T (°C)[1]	pH
1	Krugloe	54°38′58″ N	64°02′09″ E	1.27	2.62	1.5	11.7	9.3
2	Lomovo	54°37′22″ N	64°01′49″ E	0.67	1.67	1.4	12.0	9.2
3	Vtoroe Zasechnoe	54°37′39″ N	63°59′36″ E	1.68	3.62	2.0	12.5	9.3
4	Pervoe Zasechnoe	54°38′06″ N	63°58′32″ E	1.39	3.14	1.1	12.5	9.0
5	Solenoe	54°39′08″ N	63°59′08″ E	1.11	2.44	2.3	12.6	9.0
6	Dolgoe	54°39′58″ N	63°59′26″ E	1.70	4.51	1.8	12.0	9.7

No.	TDS (g\L)	DOC (mg/L)	DIC (mg/L)	Mg^{2+} (mg/L)	Ca^{2+} (mg/L)	Na^+ (mg/L)	K^+ (mg/L)	Cl^- (mg/L)	SO_4^{2-} (mg/L)	Mg/Ca Molar Ratio
1	40.2	112	343	170	30	9127	158	13,568	309	9.3
2	45.1	102	365	643	23	11,226	139	11,631	8731	46.1
3	65.1	95	275	1391	23	15,467	188	22,136	5645	99.7
4	40	69	272	827	36	8630	111	12,606	3133	37.9
5	83.5	100	240	2077	52	19,955	273	27,896	8754	65.9
6	27.7	88	355	249	7	6168	120	8809	330	58.7

[1] Sampled on 29 September 2018.

3.2. XRD Analysis of Minerals from Algae Mats and Microbialites from Vtoroe Zasechnoe Lake

The diffractograms of the most representative samples of microbialites (a) and algal mats (b) are presented in Figure 3. The interpretation of the XRD analysis results was quite difficult because the bottom sediments of Vtoroe Zasechnoye Lake are comprised of sands cemented with carbonates containing a significant amount of terrigenous components, mainly quartz and feldspars. This prevented the accurate determination of minor phases. Hydromagnesite (up to 13% ± 1%) was found in all samples of microbialites formed in shallow water. The XRD patterns, according to Reference [63], were used for the interpretation of the appearance of this hydrous Mg carbonate. Dolomite in small quantities was also likely present in one microbialites sample. Note that samples representing algae mats contained loeweite ($Na_4Mg_2(SO_4)\cdot4.5\,H_2O$), a typical mineral of marine and continental evaporate sediments [64], along with more common halite.
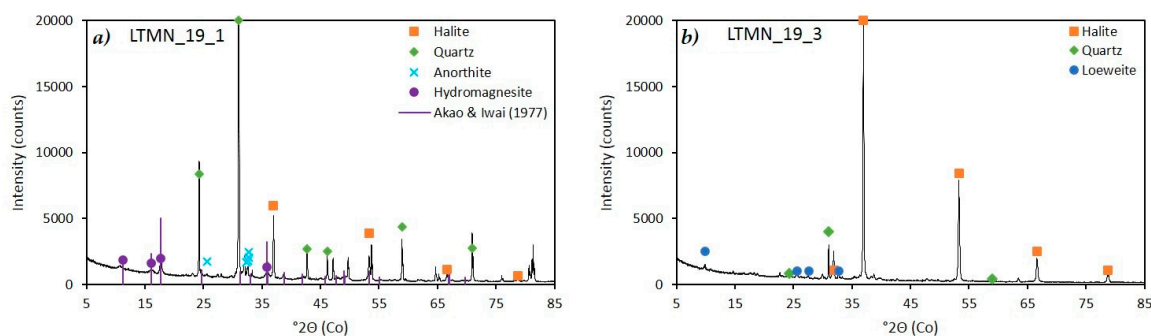
Figure 3. X-ray diffraction (XRD) patterns of representative samples of Vtoroe Zasechnoe near-shore facies: (**a**) Microbialites of the coastal zone and (**b**) dry algae mats.

3.3. Hydrogeochemical Modeling

Calculations of saturation indexes (SI) for all reservoirs of the Setovskiye group using the Visual MINTEQ software package showed (Table 2) that all the lakes are supersaturated with respect to huntite (SI > 4.52), ordered dolomite (SI > 3.89), non-ordered dolomite (SI > 3.28), magnesite (SI > 1.74), calcite (SI > 1.05), and aragonite (SI > 0.89). At the same time, with respect to monohydrocalcite, supersaturation was only observed for the least mineralized reservoir—Lake Krugloe (SI = 0.16). All studied reservoirs were undersaturated with respect to nesquehonite (SI ≤ −0.75). It is important to mention that the highest water saturation with respect to Mg-carbonates (huntite, hydromagnesite, and magnesite) was observed for the lakes Vtoroe Zasechnoe, where signs of biomineralization were found in the coastal zone and Solenoe Lake where the occurrence of Mg-carbonates was also previously reported [33]. However, one should keep the possible strong temporal heterogeneity of the Setovskiye group of water bodies in mind, since the lakes of the forest-steppe zone of Trans-Urals are subjected to significant fluctuations in the water levels within the seasons, which can affect strong variations of SI values during the year.

Table 2. Saturation indices for selected minerals, calculated with Visual MINTEQ for studied lakes.

| Minerals	Krugloe	Lomovo	Vtoroe Zasechnoe	Pervoe Zasechnoe	Solenoe	Dolgoe
	1	2	3	4	5	6
Calcite $CaCO_3$	1.51	1.13	1.05	1.2	1.31	1.1
Aragonite $CaCO_3$	1.35	0.98	0.89	1.05	1.15	0.95
Monohydrocalcite $CaCO_3 \cdot H_2O$	0.16	−0.21	−0.31	−0.14	−0.05	−0.24
Disordered dolomite $CaMg(CO_3)_2$	3.36	3.28	3.43	3.33	3.83	3.36
Ordered dolomite $CaMg(CO_3)_2$	3.97	3.89	4.03	3.93	4.45	3.97
Huntite $Mg_3Ca(CO_3)_4$	4.52	5.01	5.62	5.00	6.12	5.31
Nesquehonite $MgCO_3 \cdot 3H_2O$	−1.43	−1.15	−0.93	−1.18	−0.75	−1.03
Hydromagnesite $Mg_5(CO_3)_4(OH)_2 \cdot 4H_2O$	−0.73	0.57	2.05	0.33	2.56	1.74
Magnesite $MgCO_3$	1.74	2.02	2.23	1.97	2.37	2.13

3.4. Characterization of Algae Mats from Near-Shore Zone of Vtoroe Zasechnoe Lake

Algae mats were found within a small sandy beach in the Southeastern part of the Vtoroe Zasechnoe Lake. The thickness of these biomats varied from 5 to 10 mm (Figure 4a). The upper surface of the algae mats was characterized by a cream-beige to white color due to the precipitation of microcrystals of evaporate minerals, mainly halite. The lower wetter surface was greenish-brown with a pink tint (Figure 4b). After drying, the algae mats retained their integrity and remained fairly strong and flexible, due to the presence of poorly mineralized algae filaments.

In transparent thin sections, the heterogeneous layered texture of algae mats related to the orientation of the algae filaments was clearly visible (Figure 4c). The layers of algae mats were cemented by massive pelitomorphic carbonate material, mainly hydromagnesite (white in reflected light). Separated carbonate aggregates were much less common; however, sometimes they were present as small solid intergrowths with diameters up to 0.6 mm, consisting of a rather dense material. Small evaporite neoformations were predominantly comprised of halite. The latter occurred as radially diverging thin needles, covering the outer surface of the algae mats (Figure 4c).

When studying algae mats using a scanning electron microscope, it can be seen that filaments oriented in one plane form the structural frame of algae mats (Figure 4d). In the upper layer, most of the filaments are mineralized, while in the lower part of the algae mats, a gradual transition from non-mineralized algae filaments to massive carbonate was observed (Figures 4e and 5). These aggregates were probably developed from already decomposed or decaying organic matter.
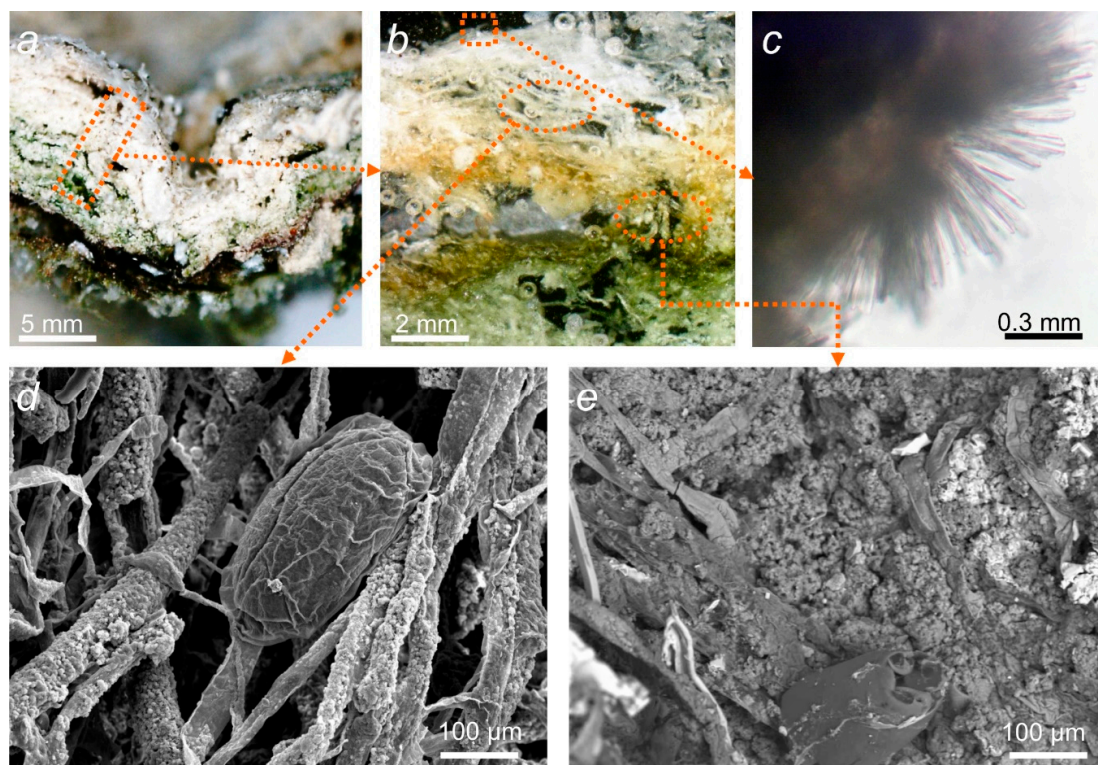
Figure 4. Microfabrics of algae mats from the near-shore zone of Vtoroe Zasechnoe Lake: (**a**) Sample with visible transition from «white» strongly mineralized with carbonate upper layers to slightly mineralized «green» bottom layer; (**b**) the same sequence in thin section (PPL); (**c**) evaporate needle crystals of halite on the surface of algae mat (PPL); (**d**) SEM image illustrating algae filaments covered with Mg-rich carbonate material in the upper mineralized layer; and (**e**) SEM image illustrating the presence of both mineralized and non-mineralized filaments in the bottom layer of the algae mat.
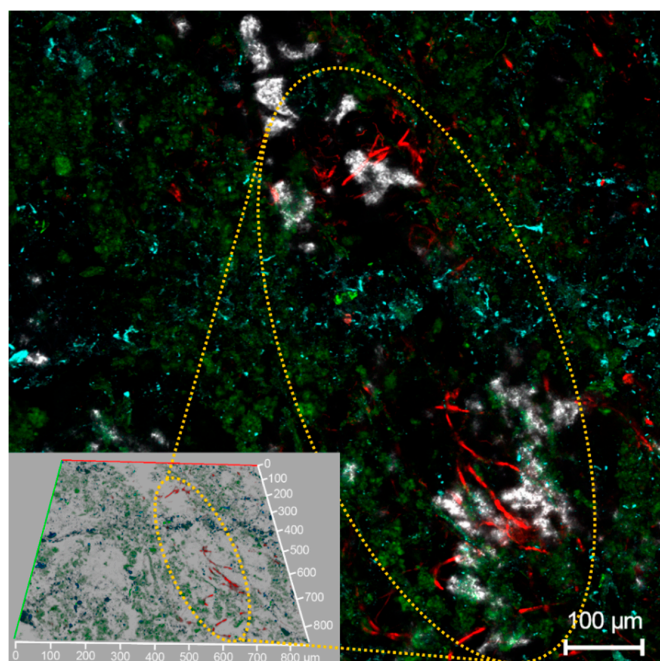
Figure 5. Confocal laser-scanning microscopy (CLSM) visualization of the middle part of the algae mat where the green color represents mineralized algae filaments and the red color corresponds to non-mineralized algae filaments.

The carbonate material that covers some of algae filaments in the mineralized parts of algae mats is represented by plate-like radially divergent crystals that formed clusters of a dumbbell or star shape (Figure 6a,b), which likely correspond to hydromagnesite, based on the morphology of crystals, their clusters, and EDS spectra. In some cases, it was clearly visible that the precipitation of carbonates occurred in areas where organic matter was degraded. Well-formed associations of crystals coexisted or developed in areas with bacterial colonies and their relics, diatom skeletons of varying degrees of preservation, and cyanobacteria and EPS films (Figure 6c,d). The evaporitic minerals on the surface of dried algae mats were represented by both very large needle-shaped microcrystals (up to 0.5 mm) revealed by the results of optical microscopy and (10–25 μm) elongated bar-shaped microcrystals of halite revealed during SEM-EDS analysis.
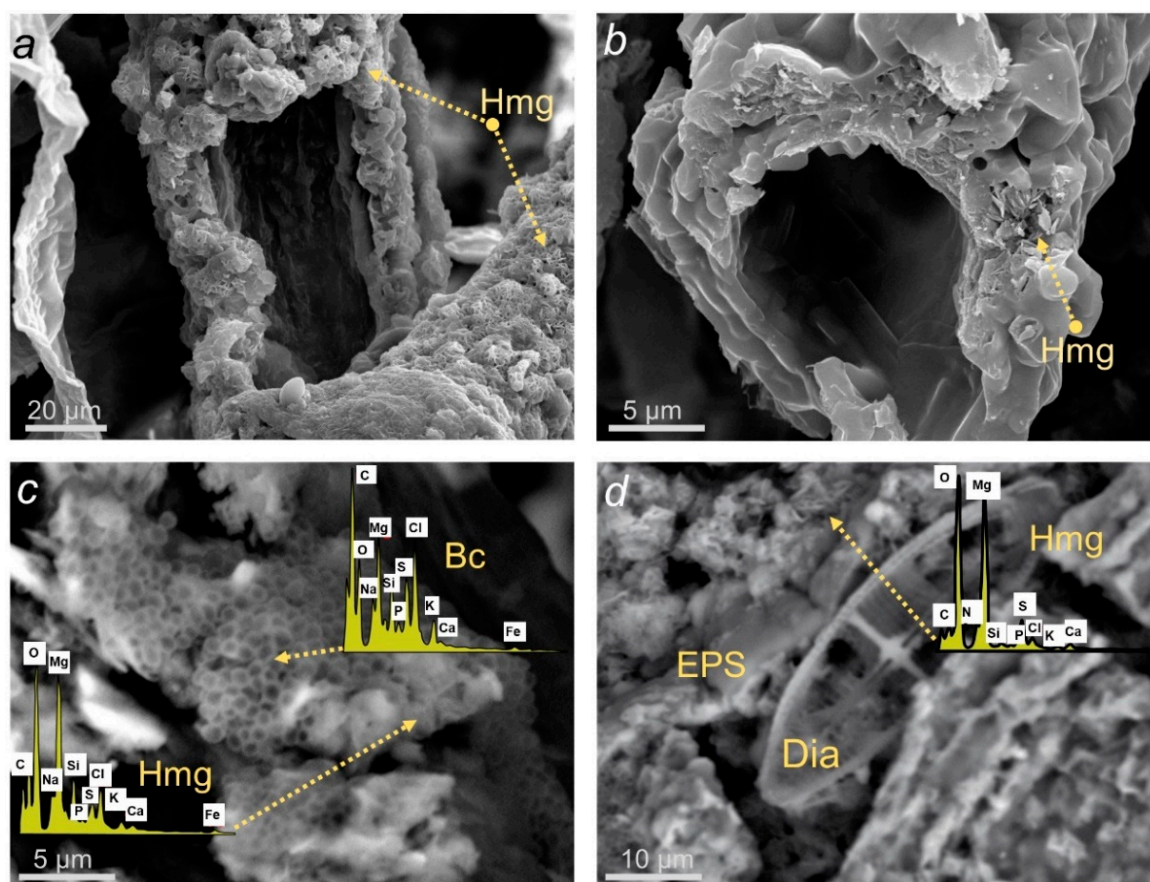

Figure 6. SEM images illustrating mineralization in algae mats: (**a**) Algae filaments covered with a massive layers of cluster plate-like crystals that likely correspond to hydromagnesite (Hmg); (**b**) bladed microcrystals (most likely hydrous Mg carbonates) developed on the mineralized filament; (**c**) transition between non-mineralized bacterial cells (Bc) and mineralized with Mg-carbonates area; and (**d**) gradual transition between mineralized and non-mineralized parts of algae mats with visible EPS films and diatom frustules (Dia).

3.5. Characterization of Initial Microbialites from the Shallow Coastal Zone of the Vtoroe Zasechnoe Lake

Microbilites are represented by thin (1–2 cm), intermittent beige-colored crusts that are unevenly distributed over the area and follow the contours of the coastline. They occurred in the shallow coastal zone of the lake, at 10–30 cm depth. After drying, the neoformations disintegrated into isometric and rather fragile pieces (Figure 7a,b). The microbialites had a laminated structure in which three separate layers can be distinguished: Upper, middle, and lower layers. The upper layer with a thickness of less than 1 mm had a lighter color and contained fewer terrigenous impurities. The middle layer

(3–5 mm thick) had a greenish color and exhibited an uneven degree of mineralization of organic matter. The lower one (4–6 mm thick) is darker in the upper part with a pinkish tinge and was largely enriched with terrigenous material, mainly quartz grains.
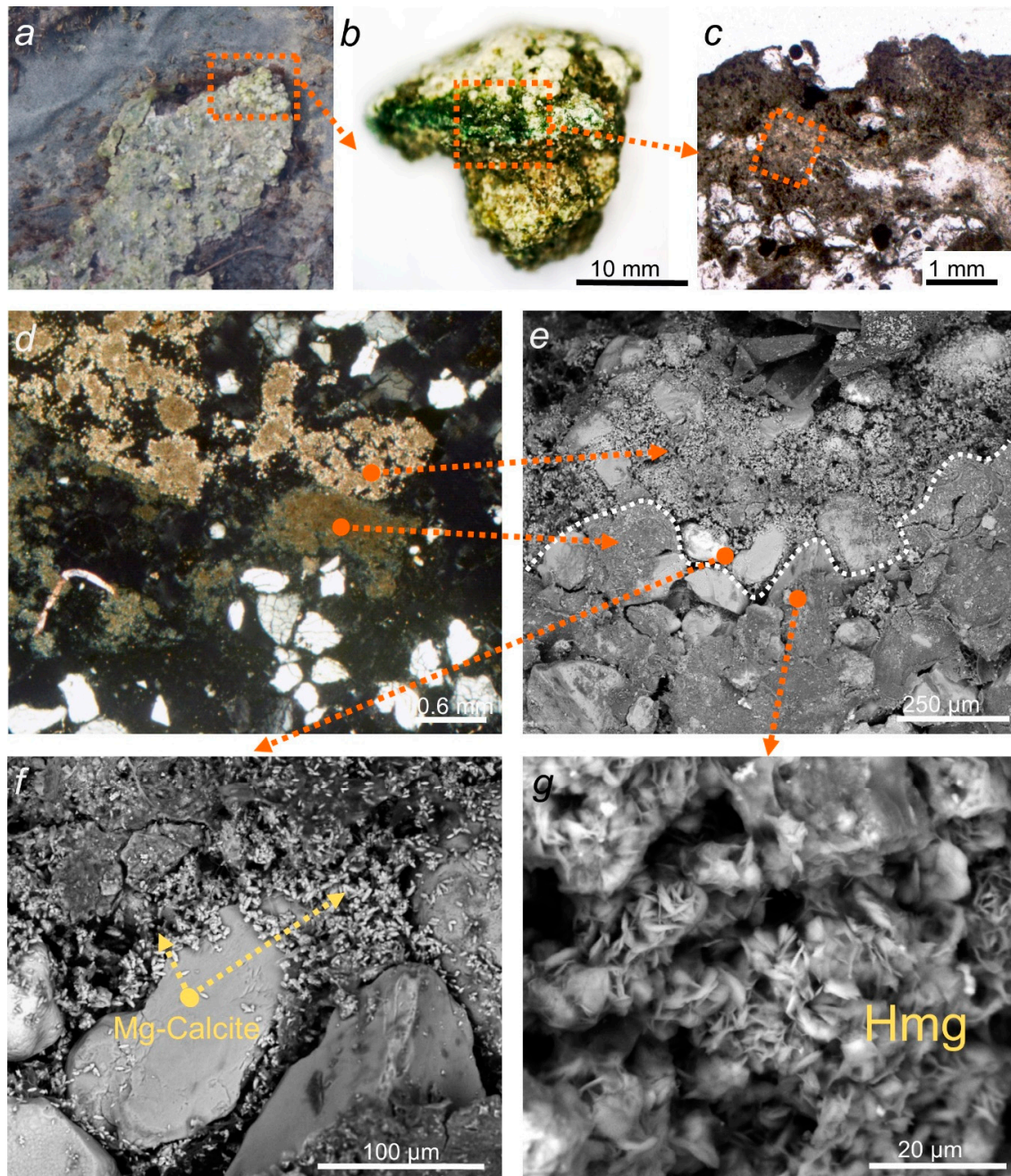

Figure 7. Structure of microbialites from near-shore zone of the Vtoroe Zasechnoe Lake: (**a**) Microbialites developed in the littoral; (**b**) layered structure of microbialites, (**c**) photograph of thin section illustrating inner structure of microbialites (PPL); (**d**) two types of layers with different carbonate minerals (XPL); (**e**) border of layers with Ca-Mg carbonates mineralization and Mg carbonates mineralization; (**f**) Ca-Mg carbonates (likely Mg-calcite microcrystals) developed in the upper loose interlayer of microbialites; and (**g**) massive Mg carbonates (probably hydromagnesite) that predominate in the more dense interlayer.

The study of microbialites in transparent thin sections using a polarizing microscope demonstrated that carbonate material is present in all the studied samples. Carbonates in the studied samples occur both as cement, and in the form of small separated aggregates. The cements consisted of small microcrystalline aggregates of carbonate minerals (up to 90%) and only in rare cases contained thin films of clay material. Two types of unevenly oriented lenticular interlayers, formed by different carbonates, can be distinguished (Figure 7c,d). One of the interlayers is enriched in dense pelitomorphic (finely crystalline) carbonate. A looser carbonate material formed aggregates consisting of slightly larger microcrystals and constituted the second type of interlayers. The terrigenous component of microbialites was mainly represented by poorly sorted quartz sand.

The SEM study of samples demonstrated that the bulk of the microbialites is a mixture of carbonate material and terrigenous particles. In this case, the terrigenous particles are enclosed in a mineral matrix, which is preserved even when individual grains fall out (Figure 8a,b). Thin mineralized films covered mineral grains and filled the space between them. Poorly mineralized residues of bacterial communities formed EPS films. In some cases, these films were covered with halite precipitations or were not mineralized at all. In most cases, the surfaces of such films were encrusted with micro-aggregates of dolomite.
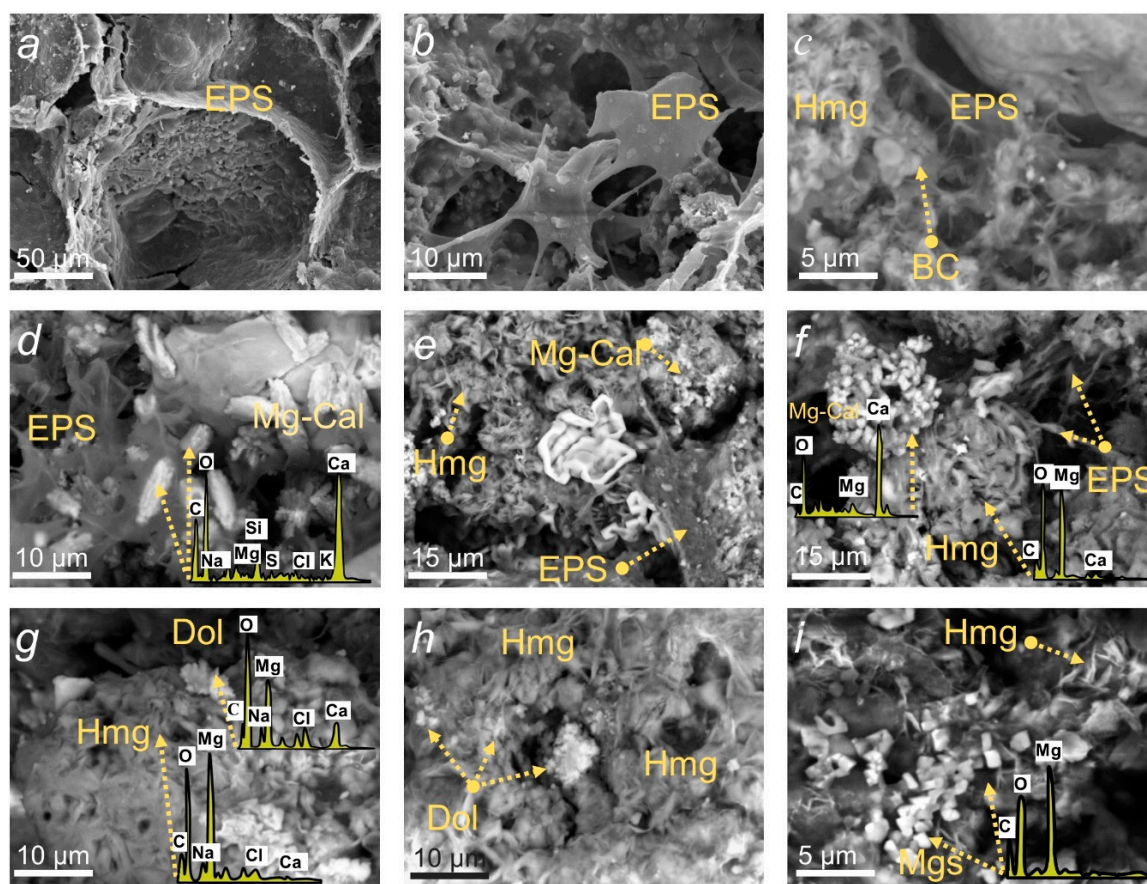
Figure 8. Mineralization of organic matric and mineral associations of microbialites: (**a**) EPS films covering terrigenous material; (**b**) EPS matrix with microcrystals developing over its surface; (**c**) Mg carbonates (probably hydromagnesite (Hmg)) developing over EPS and mineralized bacterial cells (BC); (**d**) Mg-calcite (Mg-Cal) sheath-like crystals developing from the EPS; (**e**) Mg-calcite developing within the mass of Mg carbonates; (**f**) association of Mg carbonates and Mg-calcite (Mg-Cal) developing from the EPS-matrix; (**g**) large Mg-Ca carbonate aggregate (probably protodolomite (Dol) developed within the mass mineralized by Mg-carbonates; (**h**) microcrystals of Mg-Ca carbonates and their aggregations developed within the mass mineralized by Mg hydrous carbonates; and (**i**) segregated rhombohedral microcrystals of Mg carbonate that could correspond to magnesite (Mgs).

Two unevenly alternating types of layers, which were clearly visible in thin sections, were also distinguished via the SEM-EDS technique (Figure 7e). These two layers had different carbonate associations and different density. Looser interlayers containing approximately equal proportions of Mg-calcite and hydromagnesite (Figure 7f) represented the first one. Mg-calcite was presumably formed solely by the mineralization of EPS films and precipitates in the form of spitted sheaf-like microcrystals (Figure 8a,c). Sometimes it formed loose spherical aggregates consisting of crystals and non-mineralized EPS films (Figure 8d–f). The biofilms were not completely replaced by carbonate material and remained a biopolymeric matrix during the formation of Mg-calcite. As a result, Mg-calcite crystals almost never coalesced and formed a very loose, weakly connected layer inside organo-mineral aggregates. The second layer within the microbialites was dominated by hydromagnesite, which often formed radiating clusters of fine-layered microcrystals. In such cases, carbonate material replaced organic matter almost completely (Figures 7g and 8c). Associations of hydromagnesite microcrystals in such interlayers exhibited a characteristic structure that inherited the initial cellular-alveolar structure of decaying EPS [11].

The dolomite typically occurred in layers with a predominance of hydromagnesite and a high degree of degradation of organic matter. This mineral was found in the form of isometric microcrystals encrusted in mineralized EPS films. Microcrystals had an angular, poorly delineated shape, while some crystals had a sub-rhombohedral shape. Dolomite micro-aggregates often appeared within the massive deposits of hydromagnesite (Figure 8f–h). It is noteworthy that the formation of dolomite microcrystals was only characteristic of voids mineralized by hydromagnesite. The formation of magnesite rhombohedral microcrystals was also observed in the mass mineralized by hydromagnesite (Figure 8i). However, unlike dolomite, this mineral was much less common.

4. Discussion

The Vtoroe Zasechnoe Lake is an extremely interesting natural environment to study the processes of the modern formation of Mg-carbonates. Unlike most forest-steppe drainless reservoirs of Southwestern Western Siberia with high alkalinity and high Mg/Ca values, the magnesium in Vtoroe Zasechnoe Lake is precipitated mainly in the form of hydromagnesite ($Mg_5(CO_3)_4(OH)_2 \cdot 4H_2O$), and not Mg-calcite or dolomite. In the upper layer of the bottom sediments and in the coastal zone of the Vtoroe Zasechnoe Lake, there are favorable conditions for the deposition of hydromagnesite due to the high concentrations of Mg^{2+}, HCO_3^-, and CO_3^{2-} ions, which cause the supersaturation of waters with respect to this mineral. However, this condition is necessary but not sufficient for the formation of Mg-carbonates; such surface water supersaturations are characteristic of a number of other water bodies in the forest-steppe zone of the Trans-Urals region, where formation of Mg-carbonates does not occur [33].

Figure 9 illustrates the relationships between dissolved inorganic carbon (DIC) concentration and Mg/Ca molar ratio for Setovskiye Lakes and other lacustrine environments of the world, where authigenic Mg-rich carbonates were also reported. The biplot shows that the DIC values in Trans-Urals forest-steppe reservoirs are significantly lower than in lakes and hydromagnesite–magnesite playas of the Cariboo Plateau, British Columbia, Canada [35,65], and similar or even a bit higher than for water bodies of the Turkish Lakes Region [66,67] and the alkaline lake Eras from Spain [68]. At the same time, the Mg/Ca molar ratios of Vtoroe Zasechnoe was rather high, especially in comparison to the Turkish Lakes and the Slime Lake of British Columbia. In total, the Mg/Ca ratios for all water bodies of the Setovskiye group were comparable or even higher than for most of the studied environments, except for some lakes and playas of the Cariboo Plateau.
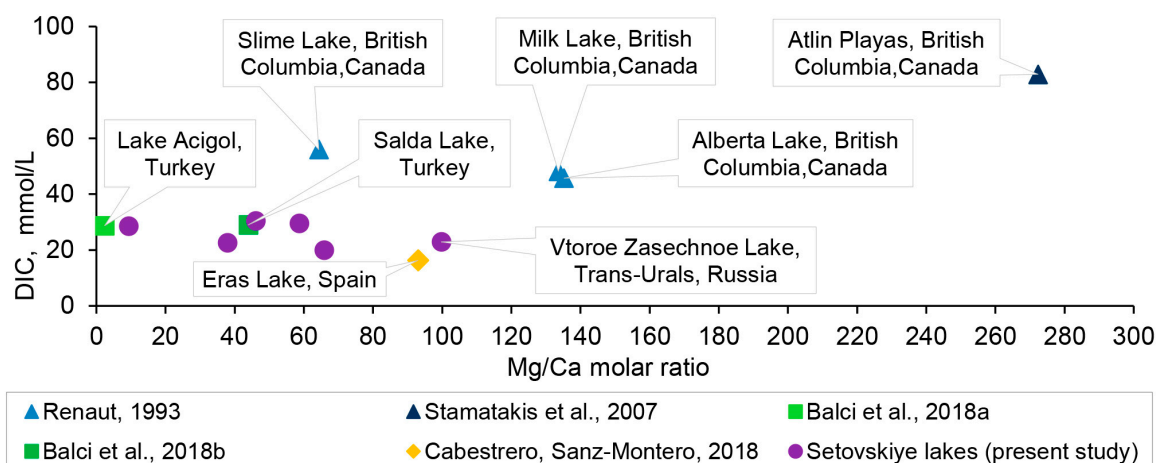
Figure 9. Biplot illustrating relationships between dissolved inorganic carbon (DIC) and Mg/Ca molar ratio for studied lakes, as well as other continental water bodies, where Mg-carbonates are formed under modern conditions collected from the published research works [35,65–68].

Accordingly, we suggest that the formation of hydromagnesite in the Vtoroe Zasechnoe Lake is related to the activity of living organisms, unique to this lake of the region. Similar to other cases of alkaline lakes, where the precipitation of Mg-carbonates prevails over Mg-Ca and Ca-carbonates [12], in the Vtoroe Zasechnoe Lake, the most intensive mineralization is confined to microbialites and algae mats in the coastal zone. This feature was also noted in previous studies of sediment cores from the Setovskiye lakes [33], where the hydromagnesite prevailed in the upper layer of bottom sediments, and sharply decreased its content with depth, due to the ceasing of phototrophic biological activity. It is therefore possible that algae, which form a dense mat of red and green color near the coastline in the summer period, are responsible for the precipitation of Mg-carbonates in Vtoroe Zasechnoe Lake. During this time of the year, intensive photosynthesis leads to the increase in the concentration of CO_3^{2-} ions and pH, creating highly supersaturated solutions, as it is known in other environments of living algal mats [25,69–72].

Another important observation is that the zones of hydromagnesite, and probably Mg-calcite and other carbonates precipitation, are confined to the degrading organic matter, such as EPS films, algae and cyanobacteria filaments, and cells of bacterial colonies. The associations of hydromagnesite microcrystals likely inherit the characteristic cellular alveolar structure of degrading EPS films [73], as is known for calcite-forming cyanobacteria [25,74]. It is possible that diatoms can play an important role in the precipitation of carbonates due to their potentially significant contribution to the formation of EPS [61,75,76]. Further, the specific features of the initial geometry of diatom frustules, having a high surface area and cation-binding sites [77], can contribute to the formation of nucleation zones via their service as templates for authigenic mineral nucleation. The skew-shaped form of Mg-calcite crystals in some cases may be related to the processes of biomineralization [12,78,79], although such mineral forms can also occur as result of abiotic precipitation [80]. For isolated microcrystals of Mg-Ca and Mg-carbonates that can correspond to dolomite and magnesite, it seems that carbonate nanoparticles, produced by bacteria in order to avoid cellular burial, act as the nucleation centers [81,82]. This mechanism was also evidenced for cyanobacteria, which possess a self-protection mechanism against calcification [83].

To sum up, the sequence of carbonate mineralization in coastal facies of the Vtorore Zasechnoe Lake can be tentatively described as follows. At the first stage, the formation of Mg-calcite occurs under the conditions of a low degree of decomposition of organic matter. At the second stage, radiating hydromagnesite microcrystals from cluster aggregates along the cellular-alveolar matrix precipitates under conditions of massive degradation of EPS. At the final stage, when organic matter

becomes deficient, Mg-Ca and Mg-carbonates microcrystals in the form of nano-globules precipitate in the vicinity of bacteria and at the cell surfaces. Recently, a similar sequence was described for the bio-mineralization of Mg-rich calcites following the degradation of microbialites in Lake Las Eras in Spain [12].

The obtained results represent the first step towards understanding the role of biomineralization processes in the formation of Mg-carbonates in forest-steppe lakes in the Southwest of Western Siberia. Further investigations should include more accurate identification of minor phases, the use of high-resolution transmission electron microscopy, and characterization of seasonal dynamics of mineralization in the Setovskiye lakes, especially the possible role of winter freezing and solute concentration in this process. These should be coupled with the assessment of genetic and metabolic diversity of specific groups of microorganisms contributing to carbonate mineral formation.

5. Conclusions

The Vtoroe Zasechnoe Lake of the forest-steppe Southwestern Western Siberia is an interesting and rare example of authigenic formation of modern hydrous Mg-carbonates. Here, we demonstrated the formation of hydromagnesite and minor Mg-Ca and Mg-carbonates, which are most likely dolomite and magnesite, in microbialites and algae mats of the coastal facies of Lake Second Zasechnoe. This lake is characterized by the highest Mg/Ca ratio among all the reservoirs of the studied group of water bodies. It is possible that this chemical environment allows for the substantial increase of solution pH during algal photosynthesis, thus creating favorable conditions for authigenic carbonate mineral formation. The association of Mg-carbonates to EPS films and bacterial cells, as well as the characteristic morphology of crystals, suggest the leading role of biomineralization processes in their formation. The obtained results represent an interesting example of the preferential precipitation of Mg-carbonates in the semiarid conditions of the Northern forest-steppe.

It is important to note that, unlike other environments for which similar processes were reported, the Setovskiye lakes are located in the conditions with rather low average annual temperatures and these shallow water bodies fully or partially freeze during winter. The role of water freezing and thawing cycles leading to solute concentration and possible oscillations of saturation degree on carbonate minerals formation in these lakes should be a subject of further studies.

References

1. Melezhik, V.A.; Fallick, A.E.; Medvedev, P.V.; Makarikhin, V.V. Palaeoproterozoic magnesite: Lithological and isotopic evidence for playa/sabkha environments. *Sedimentology* **2001**, *48*, 379–397. [CrossRef]
2. Slaughter, M.; Hill, R.J. The influence of organic-matter in organogenic dolomitization. *J. Sediment. Res.* **1991**, *61*, 296–303. [CrossRef]
3. Vasconcelos, C.; McKenzie, J.A.; Bernasconi, S.; Grujic, D.; Tiens, A.J. Microbial mediation as a possible mechanism for natural dolomite formation at low temperatures. *Nature* **1995**, *377*, 220–222. [CrossRef]
4. Vasconcelos, C.; McKenzie, J.A. Microbial mediation of modern dolomite precipitation and diagenesis under anoxic conditions (Lagoa Vermelha, Rio de Janeiro, Brazil). *J. Sediment. Res.* **1997**, *67*, 378–390. [CrossRef]

5. Land, L.S. Failure to precipitate dolomite at 25 °C from dilute solution despite 1000-fold oversaturation after 32 years. *Aquat. Geochem.* **1998**, *4*, 361–368. [CrossRef]

6. Deelman, J.C. Low-temperature nucleation of magnesite and dolomite. *Neues Jahrb. Miner. Mon.* **1999**, *7*, 289–302.

7. Königsberger, E.; Königsberger, L.; Gamsjager, H. Low-temperature thermodynamic model for the system Na_2CO_3-$MgCO_3$-$CaCO_3$-H_2O. *Geochim. Cosmochim. Acta* **1999**, *63*, 3105–3119. [CrossRef]

8. Hänchen, M.; Prigiobbe, V.; Baciocchi, R.; Mazzotti, M. Precipitation in the Mg-carbonate system – effects of temperature and CO_2 pressure. *Chem. Eng. Sci.* **2008**, *63*, 1012–1028. [CrossRef]

9. Power, I.M.; Dipple, G.M.; Francis, P.S. Assessing the carbon sequestration potential of magnesium oxychloride cement building materials. *Cem. Concr. Compos.* **2017**, *78*, 97–107. [CrossRef]

10. Power, I.M.; Kenward, P.A.; Dipple, G.M.; Raudsepp, M. Room Temperature Magnesite Precipitation. *Cryst. Growth Des.* **2017**, *17*, 5652–5659. [CrossRef]

11. Sanz-Montero, M.E.; Rodríguez-Aranda, J.P. Magnesite formation by microbial activity: Evidence from a Miocene hypersaline lake. *Sediment. Geol.* **2012**, *263*, 6–15. [CrossRef]

12. Sanz-Montero, M.E.; Cabestrero, Ó.; Sánchez-Román, M. Microbial Mg-rich Carbonates in an Extreme Alkaline Lake (Las Eras, Central Spain). *Front. Microbiol.* **2019**, *10*, 148. [CrossRef] [PubMed]

13. dos Anjos, A.P.A.; Sifeddine, A.; Sanders, C.J.; Patchineelam, S.R. Synthesis of magnesite at low temperature. *Carbonates Evaporites* **2011**, *26*, 213–215. [CrossRef]

14. Power, I.M.; Harrison, A.L.; Dipple, G.M.; Wilson, S.A.; Barker, S.L.L.; Fallon, S.J. Magnesite formation in playa environments near Atlin, British Columbia, Canada. *Geochim. Cosmochim. Acta* **2019**, *255*, 1–24. [CrossRef]

15. Braithwaite, C.J.R.; Zedef, V. Living hydromagnesite stromatolites from Turkey. *Sediment. Geol.* **1994**, *92*, 1–5. [CrossRef]

16. Shirokova, L.S.; Mavromatis, V.; Bundeleva, I.A.; Pokrovsky, O.S.; Benezeth, P.; Gerard, E.; Pearce, C.R.; Oelkers, E.H. Using Mg isotopes to trace cyanobacterially mediated magnesium carbonate precipitation in alkaline lakes. *Aquat. Geochem.* **2013**, *19*, 1–24. [CrossRef]

17. Shirokova, L.S.; Mavromatis, V.; Bundeleva, I.; Pokrovsky, O.S.; Bénézeth, P.; Pearce, C.R.; Gérard, E.; Balor, S.; Oelkers, E.H. Can Mg isotopes be used to trace cyanobacteria-mediated magnesium carbonate precipitation in alkaline lakes? *Biogeosci. Discuss.* **2011**, *8*, 6473–6517. [CrossRef]

18. Mavromatis, V.; Pearce, C.R.; Shirokova, L.S.; Bundeleva, I.A.; Pokrovsky, O.S.; Benezeth, P.; Oelkers, E.H. Magnesium isotope fractionation during hydrous magnesium carbonate precipitation with and without cyanobacteria. *Geochim. Cosmochim. Acta* **2012**, *76*, 161–174. [CrossRef]

19. Warthmann, R.; van Lith, Y.; Vasconcelos, C.; McKenzie, J.A.; Karpoff, A.M. Bacterially induced dolomite precipitation in anoxic culture experiments. *Geology* **2000**, *28*, 1091–1094. [CrossRef]

20. Roberts, J.A.; Bennett, P.C.; Gonzalez, L.A.; Macpherson, G.L.; Miliken, K.L. Microbial precipitation of dolomite in methanogenic groundwater. *Geology* **2004**, *32*, 277–280. [CrossRef]

21. Sánchez-Román, M.; Vasconcelos, C.; Warthmann, R.; Rivadeneyra, M.; McKenzie, J.A. Microbial dolomite precipitation under aerobic conditions: Results from Brejo do Espinho Lagoon (Brazil) and Culture Experiments. In *Perspectives in Carbonate Geology: A Tribute to the Career of Robert Nathan Ginsburg*; Swart, P.K., Eberli, G.P., McKenzie, J.A., Jarvis, I., Stevens, T., Eds.; Blackwell Publishing: Chichester, UK, 2009; Volume 41, pp. 167–178. [CrossRef]

22. Deng, S.; Dong, H.; Lv, G.; Jiang, H.; Yu, B.; Bishop, M.E. Microbial dolomite precipitation using sulfate reducing and halophilic bacteria: Results from Qinghai Lake, Tibetan Plateau, NW China. *Chem. Geol.* **2010**, *278*, 151–159. [CrossRef]

23. Dittrich, M.; Sibler, S. Calcium Carbonate Precipitation by Cyanobacterial Polysaccharides. In *Tufas and Speleothems: Unravelling the Microbial and Physical Controls*; Pedley, H.M., Rogerson, M., Eds.; Geological Society London Special Publication: London, UK, 2010; Volume 336, pp. 51–63. [CrossRef]

24. Bundeleva, I.A.; Shirokova, L.S.; Bénézeth, P.; Pokrovsky, O.S.; Kompantseva, E.I.; Balor, S. Calcium carbonate precipitation by anoxygenic phototrophic bacteria. *Chem. Geol.* **2012**, *291*, 116–131. [CrossRef]

25. Bundeleva, I.A.; Shirokova, L.S.; Pokrovsky, O.S.; Bénézeth, P.; Ménez, B.; Gérard, E.; Balor, S. Experimental modeling of calcium carbonate precipitation by cyanobacterium *Gloeocapsa* sp. *Chem. Geol.* **2014**, *374–375*, 44–60. [CrossRef]

26. Al Disi, Z.A.; Jaoua, S.; Bontognali, T.R.R.; Attia, E.S.M.; Al-Kuwari, H.A.A.S.; Zouari, N. Evidence of a Role for Aerobic Bacteria in High Magnesium Carbonate Formation in the Evaporitic Environment of Dohat Faishakh Sabkha in Qatar. *Front. Environ. Sci.* **2017**, *5*. [CrossRef]

27. DiLoreto, Z.A.; Bontognali, T.R.R.; Al Disi, Z.A.; Al-Kuwari, H.A.S.; Williford, K.H.; Strohmenger, C.J.; Sadooni, F.; Palermo, C.; Rivers, J.M.; McKenzie, J.A.; et al. Microbial community composition and dolomite formation in the hypersaline microbial mats of the Khor Al-Adaid sabkhas, Qatar. *Extremophiles* **2019**, *23*, 201–218. [CrossRef]

28. Power, I.M.; Wilson, S.A.; Thom, J.M.; Dipple, G.M.; Gabites, J.E.; Southam, G. The hydromagnesite playas of Atlin, British Columbia, Canada: A biogeochemical model for CO_2 sequestration. *Chem. Geol.* **2009**, *260*, 286–300. [CrossRef]

29. McCutcheon, J.; Power, I.M.; Harrison, A.L.; Dipple, G.M.; Southam, G. A greenhouse-scale photosynthetic microbial bioreactor for carbon sequestration in magnesium carbonate minerals. *Environ. Sci. Technol.* **2014**, *48*, 9142–9151. [CrossRef]

30. McCutcheon, J.; Power, I.M.; Shuster, J.; Harrison, A.L.; Dipple, G.M.; Southam, G. Carbon Sequestration in Biogenic Magnesite and Other Magnesium Carbonate Minerals. *Environ. Sci. Technol.* **2019**, *53*, 3225–3237. [CrossRef]

31. Alderman, A.R.; von der Borch, C.C. Occurrence of Hydromagnesite in Sediments in South Australia. *Nature* **1960**, *188*, 931. [CrossRef]

32. Pueyo, J.; Inglés, M. Substrate mineralogy, interstitial brine composition and diagenetic processes in the playa lakes of Los Monegros and Bajo Aragón (Spain). In *Geochemistry and Mineral Formation in the Earth Surface, Proceedings of the International Meeting "Geochemistry of the Earth Surface and Processes of Mineral Formation", Granada, Spain, 16–22 March 1986*; Rodriguez-Clemente, R., Tardy, Y., Eds.; Centre National de la Researche Scientifique: Paris, France, 1987; pp. 351–372.

33. Shlyapnikov, D.S.; Demchuk, N.G.; Okunev, P.V. *Mineral Components of Bottom Sediments of the Lakes of the Urals*; Ural State University: Sverdlovsk, Russia, 1990. (In Russian)

34. Last, W.M. Petrology of modern carbonate hardgrounds from East Basin Lake, a Saline Maar Lake, Southern Australia. *Sediment. Geol.* **1992**, *81*, 215–229. [CrossRef]

35. Renaut, R.W. Morphology, distribution, and preservation potential of microbial mats in the hydromagnesite-magnesite playas of the Cariboo Plateau, British-Columbia, Canada. *Hydrobiologia* **1993**, *267*, 75–98. [CrossRef]

36. Braithwaite, C.J.R.; Zedef, V. Hydromagnesite stromatolites and sediments in an alkaline lake, Salda Golu, Turkey. *J. Sediment. Res.* **1996**, *66*, 991–1002. [CrossRef]

37. Queralt, I.; Julia, R.; Plana, F.; Bischoff, J.L. A hydrous Ca-bearing magnesium carbonate from playa lake sediments, Saline Lake, Spain. *Am. Mineral.* **1997**, *82*, 812–819. [CrossRef]

38. Coshell, L.; Rosen, M.R.; McNamara, K.J. Hydromagnesite replacement of biomineralized aragonite in a new location of Holocene stromatolites, Lake Walyungup, Western Australia. *Sedimentology* **1998**, *45*, 1005–1018. [CrossRef]

39. Kaźmierczak, J.; Kempe, S.; Kremer, B.; López-García, P.; Moreira, D.; Tavera, R. Hydrochemistry and microbialites of the alkaline crater lake Alchichica, Mexico. *Facies* **2011**, *57*, 543–570. [CrossRef]

40. Last, F.M.; Last, W.M. Lacustrine carbonates of the northern Great Plains of Canada. *Sediment. Geol.* **2012**, *277*, 1–31. [CrossRef]

41. Couradeau, E.; Benzerara, K.; Gérard, E.; Estève, I.; Moreira, D.; Tavera, R.; López-García, P. Cyanobacterial calcification in modern microbialites submicrometer scale. *Biogeosciences* **2013**, *10*, 5255–5266. [CrossRef]

42. Power, I.M.; Wilson, S.A.; Harrison, A.L.; Dipple, G.M.; McCutcheon, J.; Southam, G.; Kenward, P.A. A depositional model for hydromagnesite–magnesite playas near Atlin, British Columbia, Canada. *Sedimentology* **2014**, *61*, 1701–1733. [CrossRef]

43. Sanz-Montero, M.E.; Cabestrero, Ó.; Rodríguez-Aranda, J. Hydromagnesite precipitation in microbial mats from a highly alkaline lake, Central Spain. *Mineral. Mag.* **2013**, *77*, 2133.

44. Lin, Y.; Zheng, M.; Ye, C. Hydromagnesite precipitation in the Alkaline Lake Dujiali, central Qinghai-Tibetan Plateau: Constraints on hydromagnesite precipitation from hydrochemistry and stable isotopes. *Appl. Geochem.* **2017**, *78*, 139–148. [CrossRef]

45. Lin, Y.; Zheng, M.; Ye, C.; Power, I.M. Rare earth element and strontium isotope geochemistry in Dujiali Lake, central Qinghai-Tibet Plateau, China: Implications for the origin of hydromagnesite deposits. *Chem. ERDE Geochem.* **2019**, *79*, 337–346. [CrossRef]

46. Power, I.M.; Wilson, S.A.; Thom, J.M.; Dipple, G.M.; Southam, G. Biologically induced mineralization of dypingite by cyanobacteria from an alkaline wetland near Atlin, British Columbia, Canada. *Geochem. Trans.* **2007**, *8*, 13. [CrossRef]

47. Alçiçek, H. Late Miocene nonmarine sedimentation and formation of magnesites in the Acigol Basin, southwestern Anatolia, Turkey. *Sediment. Geol.* **2009**, *219*, 115–135. [CrossRef]

48. Tkachev, B.P. *Inland Regions of the South of Western Siberia*; Tomsk State University Publication: Tomsk, Russia, 2001. (In Russian)

49. Strakhovenko, V.D.; Solotchina, E.P.; Vosel', Y.S.; Solotchin, P.A. Geochemical factors for endogenic mineral formation in the bottom sediments of the Tazheran lakes (Baikal area). *Russ. Geol. Geophys.* **2015**, *56*, 1437–1450. [CrossRef]

50. Samylina, O.S.; Zaytseva, L.V.; Sinetova, M.A. Participation of algal–bacterial community in the formation of modern stromatolites in Cock Soda Lake, Altai Region. *Paleontol. J.* **2016**, *50*, 635–645. [CrossRef]

51. Gaskova, O.L.; Strakhovenko, V.D.; Ovdina, E.A. Composition of brines and mineral zoning of the bottom sediments of soda lakes in the Kulunda steppe (West Siberia). *Russ. Geol. Geophys.* **2017**, *58*, 1199–1210. [CrossRef]

52. Samylina, O.S.; Zaytseva, L.V. Characterization of modern dolomite stromatolites from hypersaline Petukhovskoe Soda Lake, Russia. *Lethaia* **2018**, *52*, 1–13. [CrossRef]

53. Kolpakova, M.N.; Gaskova, O.L.; Naymushina, O.S.; Karpov, A.V.; Vladimirov, A.G.; Krivonogov, S.K. Saline lakes of Northern Kazakhstan: Geochemical correlations of elements and controls on their accumulation in water and bottom sediments. *Appl. Geochem.* **2019**, *107*, 8–18. [CrossRef]

54. Strakhovenko, V.; Ovdina, E.; Solotchina, E.; Malov, G. Features of formation of authigenic minerals in holocene bottom sediments of small lakes of Western Siberia. In *Paleolimnology of Northern Eurasia: Experience, Methodology, Current Status and Young Scientists School in Microscopy Skills in Paleolimnology, Proceedings of the 3rd International conference, Kazan, Republic of Tatarstan, Russia, 1–4 October 2018*; Frolova, L.A., Ibragimova, A.G., Nigamatzyanova, G.R., Eds.; Publishing House of Kazan University: Kazan, Russia, 2018; pp. 119–123.

55. Zemtsov, A.A. *Geomorphology of the West Siberian Plain*; Tomsk State University Publication: Tomsk, Russia, 1976. (In Russian)

56. Puzhakov, B.A.; Saveliev, V.P.; Kuznetsov, N.S.; Shokh, V.D.; Schulkin, E.P.; Schulkina, N.E.; Zhdanov, A.V.; Dolgova, O.Y.; Tarelkina, E.A.; Orlov, M.V. Explanatory note. In *State Geological Map of the Russian Federation. Scale 1: 1,000,000 (Third Generation)*; Series Ural. Sheet N41—Chelyabinsk; Zotova, E.A., Ed.; Cartographic factory VSEGEI: St. Petersburg, Russia, 2013. (In Russian)

57. Climate-Data.org. Available online: https://ru.climate-data.org/азия/россииская-федерация/курганская-область/куртамыш-59573/ (accessed on 26 September 2019).

58. Konstantinova, E.Y. Trace metals in soils of the main geomorphological units in the southwestern part of Western Siberia. *Earth Environ.* **2016**, *43*, 012002. [CrossRef]

59. Pokrovsky, O.S.; Shirokova, L.S.; Kirpotin, S.N.; Audry, S.; Viers, J.; Dupré, B. Effect of permafrost thawing on organic carbon and trace element colloidal speciation in the thermokarst lakes of western Siberia. *Biogeosciences* **2011**, *8*, 565–583. [CrossRef]

60. Pace, A.; Bourillot, R.; Bouton, A.; Vennin, E.; Braissant, O.; Dupraz, C.; Duteil, T.; Bundeleva, I.; Patrier, P.; Galaup, S.; et al. Formation of stromatolite lamina at the interface of oxygenic–anoxygenic photosynthesis. *Geobiology* **2018**, *16*, 378–398. [CrossRef] [PubMed]

61. Payandi-Rolland, D.; Roche, A.; Vennin, E.; Visscher, P.T.; Amiotte-Suchet, P.; Thomas, C.; Bundeleva, I.A. Carbonate Precipitation in Mixed Cyanobacterial Biofilms Forming Freshwater Microbial Tufa. *Minerals* **2019**, *9*, 409. [CrossRef]

62. Visual MINTEQ. Available online: https://vminteq.lwr.kth.se (accessed on 30 June 2019).

63. Akao, M.; Iwai, S. The hydrogen bonding of hydromagnesite. *Acta Cryst. B* **1977**, *33*, 1273–1275. [CrossRef]

64. Roberts, W.L.; Campbell, T.J.; Rapp, G.R. *Encyclopedia of Minerals*, 2nd ed.; Chapman & Hall: New York, NY, USA, 1990.

65. Stamatakis, M.G.; Renaut, R.W.; Kostakis, K.; Tsivilis, S.; Stamatakis, G.; Kakali, G. The hydromagnesite deposits of the Atlin area, British Columbia, Canada, and their industrial potential as a fire retardant. *Bull. Geol. Soc. Greece* **2007**, *40*, 972–983. [CrossRef]

66. Balci, N.; Demirel, C.; Akcer Ön, S.; Gültekin, A.H.; Kurt, M.A. Evaluating abiotic and microbial factors on carbonate precipitation in Lake Acigöl, a hypersaline lake in Southwestern Turkey. *Quatern. Int.* **2018**, *486*, 116–128. [CrossRef]

67. Balci, N.; Demirel, C.; Kurt, M.A. Geomicrobiology of Lake Salda and microbial influences on present-day stromatolite formation. *Yerbilimleri* **2018**, *39*, 19–40. (In Turkish)

68. Cabestrero, Ó.; Sanz-Montero, M.E. Brine evolution in two inland evaporative environments: Influence of microbial mats in mineral precipitation. *J. Paleolimnol.* **2018**, *59*, 139–157. [CrossRef]

69. Dubinsky, Z.; Rotem, J. Relations between algal populations and the pH of their media. *Oecologia* **1974**, *16*, 53–60. [CrossRef]

70. Merz, M.U.E.; Schlue, W.R.; Zankl, H. pH-Measurement in the sheath of calcifying filamentous cyanobacteria. *Bull. Inst. Oceanogr.* **1995**, *14*, 281–289.

71. Arp, G.; Bissett, A.; Brinkmann, N.; Cousin, S.; De Beer, D.; Friedl, T.; Mohr, K.I.; Neu, T.R.; Reimer, A.; Shiraishi, F.; et al. Tufa-Forming Biofilms of German Karstwater Streams: Microorganisms, Exopolymers, Hydrochemistry and Calcification. In *Tufas and Speleothems: Unravelling the Microbial and Physical Controls*; Pedley, H.M., Rogerson, M., Eds.; Geological Society London Special Publications: London, UK, 2010; Volume 336, pp. 83–118. [CrossRef]

72. Shiraishi, F. Chemical conditions favoring photosynthesis-induced $CaCO_3$ precipitation and implications for microbial carbonate formation in the ancient ocean. *Geochim. Cosmochim. Acta* **2012**, *77*, 157–174. [CrossRef]

73. Trichet, J.; Defarge, C.; Tribble, J.; Tribble, G.; Sansone, F. Christmas Island lagoonal lakes, models for the deposition of carbonate-evaporite organic laminated sediments. *Sediment. Geol.* **2001**, *140*, 177–189. [CrossRef]

74. Obst, M.; Dynes, J.J.; Lawrence, J.R.; Swerhone, G.D.W.; Benzerara, K.; Karundakaran, C.; Kaznatcheev, K.; Tyliszcak, T.; Hitchcock, A.P. Precipitation of amorphous $CaCO_3$ (aragonite-like) by cyanobacteria: A STXM study of the influence of EPS on the nucleation process. *Geochim. Cosmochim. Acta* **2009**, *73*, 4180–4198. [CrossRef]

75. Decho, A.W. Exopolymer Microdomains as a Structuring Agent for Heterogeneity within Microbial Biofilms. In *Microbial Sediments*; Riding, R.E., Awramik, S.M., Eds.; Springer: Berlin/Heidelberg, Germany, 2000; pp. 9–15. [CrossRef]

76. Roche, A.; Vennin, E.; Bundeleva, I.; Bouton, A.; Payandi-Rolland, D.; Amiotte-Suchet, P.; Gaucher, E.C.; Courvoisier, H.; Visscher, P.T. The Role of the Substrate on the Mineralization Potential of Microbial Mats in A Modern Freshwater River (Paris Basin, France). *Minerals* **2019**, *9*, 359. [CrossRef]

77. Gelabert, A.; Pokrovsky, O.S.; Schott, J.; Boudou, A.; Fertet-Mazel, A.; Mielczarski, E.; Mielczarski, J.; Spalla, O. Study of diatoms/aqueous solution interface. I. Acid-base equilibria, surface charge and spectroscopic observation of two freshwater peryphytic and two marine planktonic diatoms. *Geochim. Cosmochim. Acta* **2004**, *68*, 4039–4058. [CrossRef]

78. Leonova, L.V.; Potapov, S.S.; Kuz'mina, L.Y.; Cherviatsova, O.Y.; Glavatskikh, S.P.; Riabova, A.S. The technogenic sediments of biocarbonates and their experimental formation. *Mineral. Tekhnogeneza* **2014**, *15*, 113–129. (In Russian)

79. Novoselov, A.; Konstantinov, A.; Leonova, L.; Soktoev, B.; Morgalev, S. Carbonate Neoformations on Modern Buildings and Engineering Structures in Tyumen City, Russia: Structural Features and Development Factors. *Geosciences* **2019**, *9*, 128. [CrossRef]

80. Xiao, J.; Yang, S. Hollow calcite crystals with complex morphologies formed from amorphous precursors and regulated by surfactant micellar structures. *CrystEngComm* **2010**, *12*, 3296–3304. [CrossRef]

81. Bontognali, T.R.R.; Vasconcelos, C.; Warthmann, R.J.; Dupraz, C.; Bernasconi, S.M.; McKenzie, J.A. Microbes produce nanobacteria-like structures, avoiding cell entombment. *Geology* **2008**, *36*, 663–666. [CrossRef]

82. Sánchez-Román, M.; Vasconcelos, C.; Schmid, T.; Dittrich, M.; McKenzie, J.A.; Zenobi, R.; Rivadeneyra, M.A. Aerobic microbial dolomite at the nanometer scale: Implications for the geologic record. *Geology* **2008**, *36*, 879–882. [CrossRef]

83. Martinez, R.; Gardes, E.; Pokrovsky, O.S.; Schott, J.; Oelkers, E.H. Do photosynthetic bacteria have a protective mechanism against carbonate precipitation at their surfaces? *Geochim. Cosmochim. Acta* **2010**, *74*, 1329–1337. [CrossRef]